

## INFRARED HETERODYNE RECEIVERS WITH IF RESPONSES APPROACHING 5 GHz\*

J.M. Wolczok and B.J. Peyton  
Eaton Corporation, AIL Division, Melville, NY 11747

### SUMMARY

Laser probing of high density tokamak plasmas has led to the development of specialized coherent 10.6  $\mu\text{m}$  infrared receivers with IF frequency responses approaching 5 GHz.  $\text{CO}_2$  lasers are employed for these applications because of their availability, stability, and high average-power levels. The use of a high-power laser probing source and a highly scattering plasma requires the use of a photomixer which can detect weak laser signals in the presence of high stray-laser levels. Accordingly, heterodyne receivers which employ extrinsic photoconductive Ge:Cu(Sb) mixers have been developed for measurements of  $\text{CO}_2$  laser scattering to determine: (1) the driven lower-hybrid wave density fluctuations, and (2) the plasma ion temperature of dense tokamak plasmas.

The liquid helium cooled Ge:Cu(Sb) detectors are operated in a high photogain mode in which the photomixer impedance is approximately 1200 ohms. This paper reports on IF impedance matching techniques which are aimed at optimizing: (1) the power transfer between the photomixer and the IF pre-amplifier, and (2) the receiver sensitivity over the IF frequency range of interest. In particular, cooled 1200 to 50 ohm impedance matching networks have been employed to optimize heterodyne receiver performance. Although this work has been carried out with Ge:Cu photomixers, these IF impedance matching techniques are also applicable to other wideband infrared photomixers, such as PV:HgCdTe.

Two relatively narrow band 10.6  $\mu\text{m}$  heterodyne receivers with IF center frequencies near 2.5 and 4.6 GHz have been developed for lower-hybrid wave density fluctuation measurements in tokamak plasmas. The 2.5 GHz response heterodyne receiver provides an NEP of  $2 \times 10^{-19}$  W/Hz for an applied dc bias power of 104 mW, while the 4.6 GHz response heterodyne receiver provides an NEP of  $4.4 \times 10^{-19}$  W/Hz for an applied dc bias power of 150 mW. A broadband 10.6  $\mu\text{m}$  heterodyne receiver has also been developed for remote ion temperature measurements of a tokamak plasma. This receiver operates over the 200 to 1300 MHz IF frequency range and provides an NEP as low as  $1.5 \times 10^{-19}$  W/Hz with an applied dc bias power of only 60 mW.

\*This work was supported by the United States Energy Research and Development Administration.

## PLASMA PROBING

CO<sub>2</sub> laser scattering of quasi-free electrons in a dense tokamak plasma (ref. 1) permits the remote determination of: (1) the amplitude and spectral and spatial distributions of driven lower-hybrid wave fluctuations (ref. 2 and 3), and (2) the plasma ion temperature (ref. 4 and 5). The use of a 100 W CW CO<sub>2</sub> laser radiation results in a forward scattering angle of about 1° and a relatively large amount (1 to 3 mW) of stray laser radiation at the infrared detector. However, the overall heterodyne sensitivity is relatively unaffected by the stray laser radiation because the diagnostic receiver utilizes: (1) transmitter and local oscillator (LO) sources which operate at the same frequency, and (2) an extrinsic photoconductive mixer which utilizes an incident laser LO level of between 50 and 100 mW (ref. 6). (It has also been suggested (ref. 7) that CO<sub>2</sub> laser diagnostics will permit the remote measurement of the poloidal-field in a tokamak plasma.)

An important method of heating tokamak plasma involves the application of RF energy which generates lower hybrid waves that propagate to the center of the plasma and deposit energy into the ions and electrons (ref. 3). At the MIT Alcator tokamak, 50 kW of CW microwave radiation is coupled into the core at a plasma wave resonant frequency of 2.5 (or 4.6) GHz (ref. 2). A coherent 100 W CO<sub>2</sub> laser beam probes the plasma to determine the depth of the RF energy penetration and a wideband heterodyne receiver has been developed for plasma diagnostic measurements. A microwave antenna is used to direct the RF radiation toward the plasma. Two CO<sub>2</sub> beams (a 100 W transmitter and a 1 W LO) from a common laser source are coupled into the plasma at right angles to the microwave radiation (fig. 1). The two laser beams are adjusted to cross in a small spatial cross-section (1 mm X 1 mm) of the plasma (ref. 8). The interaction of the microwave radiation and the transmit laser beam in the nonlinear plasma results in both a spatial and Doppler spectral shift in the transmitter laser radiation. The shifted laser beam and the unshifted laser LO beam are spatially aligned to fall on the wideband photomixer. The measured intensity of the frequency shifted (2.5 or 4.6 GHz offset) laser beam across the plasma provides information on the RF mismatch at the turbulent vacuum-plasma boundary layer, and the measured frequency spread of the shifted laser beam provides information on the boundary layer physics.

The ion temperature measurement setup employs a pulsed CO<sub>2</sub> laser beam with a peak transmit power level near  $5 \times 10^5$  W. From a single particle perspective, the electrons radiate a Doppler shifted frequency which is related to its velocity compared to the incident and scattered laser beams. The average of all such scattering events leads to a scattered spectrum whose width is related to the plasma ion temperature. The actual average Doppler shift is due to the ion motion in the plasma rather than the electron motion because the laser scattering is from the electron shield that surrounds each ion. The width of the scattered spectrum in the 300 to 1300 MHz frequency range is determined using IF channelizer techniques.

## HETERODYNE RECEIVER DESIGN

The sensitivity (NEP) and the available conversion gain (G) for an infrared heterodyne receiver which uses an extrinsic photoconductive mixer are given (ref. 9) by

$$\text{NEP} = \frac{2h\nu B}{\eta} + \frac{k (T_m + T'_{IF}) B}{GC} = \frac{2h\nu B}{\eta'} \quad (1)$$

$$G = \frac{\eta q V}{2h\nu} \left( \frac{\tau}{T} \right) \frac{1}{1 + \omega^2 \tau^2} \quad (2)$$

where  $h$  is Planck's constant,  $\nu$  is the infrared frequency,  $B$  is the IF bandwidth,  $\eta$  is the photomixer quantum efficiency,  $k$  is Boltzmann's constant,  $T_m$  is the photomixer temperature,  $T'_{IF}$  is the effective IF amplifier noise figure,  $C$  is the IF impedance matching efficiency,  $\eta'$  is the effective heterodyne quantum efficiency,  $q$  is the electronic charge,  $V$  is the mixer bias voltage,  $\tau$  is the photomixer carrier lifetime,  $T$  is the photomixer transit time, and  $\omega$  is the angular IF frequency.

Optimum heterodyne receiver performance is achieved by minimizing the thermal noise term in equation (1). This term can be minimized by: (1) using a low noise IF preamplifier, (2) increasing the photomixer gain, and (3) maximizing the impedance matching efficiency by using a matching network.

The photomixer conversion gain [equation (2)] can be increased by increasing the applied dc bias voltage. However, the photomixer must be operated in a linear portion of its current-voltage (I-V) characteristic. It should be noted that the photomixer transit time varies directly with the photomixer interelectrode spacing and inversely with the applied bias voltage. The  $(1 + \omega^2 \tau^2)^{-1}$  term in equation (2) represents the finite photomixer IF frequency response.

The photomixer IF output resistance,  $R_o$ , is given (ref. 8) by

$$R_o = \frac{L^2 h\nu_{LO}}{q\mu\eta P_{LO}} \quad (3)$$

where  $L$  is the photomixer interelectrode spacing,  $\mu$  is the mobility of principal carriers, and  $P_{LO}$  is the incident laser LO power. As can be seen, the photomixer IF output resistance varies inversely as the square of the photomixer interelectrode spacing. Accordingly, a photomixer height of  $L = 250 \mu\text{m}$  was selected for the plasma probing applications to: (1) ease the impedance matching network requirements, and (2) increase the photomixer gain by decreasing the photomixer transit time.

Substituting equation (3) into equation (2), the photomixer conversion gain is

$$G = \frac{P_{dc}}{2P_{LO}} \left( \frac{1}{1 + \omega^2 \tau^2} \right) \quad (4)$$

From equations (3) and (4), the photomixer gain and the photomixer resistance both increase inversely with LO power. Therefore, a tradeoff is required to select the incident laser LO power level which will result in sufficient overall photomixer gain and a photomixer resistance which can be efficiently matched to the 50-ohm IF preamplifier. The photomixer resistance is typically 12 megohms with no incident LO power and is reduced to approximately 1200 ohms with applied laser LO power. A cooled microwave impedance matching network is used to obtain nearly optimum power transfer between the photomixer and IF preamplifier over the IF frequency range of interest.

#### Ge:Cu(Sb) PHOTOMIXERS

As has been mentioned, wideband extrinsic germanium photomixers are used for CO<sub>2</sub> laser plasma probing diagnostics because the stray laser radiation would saturate and possibly damage available wideband PV:HgCdTe photomixers. Measured carrier lifetimes of Ge:Au and Ge:Cu photomixers are given in figure 2. As can be seen, the carrier lifetime varies with donor concentration and applied electric field (ref. 10, 11, and 12). Typical Ge:Cu characteristics for a highly doped photomixer which exhibits wideband performance are given in table I. To our knowledge, this photomixer cutoff frequency (set by the carrier lifetime) is the highest value reported for Ge:Cu(Sb) photomixers. The photomixer IF response is flat to 300 MHz, 3-dB down at 800 MHz, and 10-dB down at 2500 MHz.

The measured photomixer I-V characteristic (fig. 3) demonstrates that an applied voltage of 15 volts, and above, can be used in the positive biasing direction to maximize the photoconductive gain [equation (2)]. For heterodyne receiver operation at lower IF frequencies, special attention must be given to minimize the contact (1/f) noise at high bias levels by utilizing good ohmic contacts.

#### IF IMPEDANCE MATCHING

It has been demonstrated (ref. 10) that wideband infrared receivers which have impedance mismatches between the photomixer output and the IF preamplifier

will exhibit significant variations in sensitivity with changing IF frequency. These sensitivity variations are exaggerated by the use of a fixed (50 ohm) impedance transmission line between the photomixer and IF preamplifier. A previously developed (ref. 13) wideband IF preamplifier was mounted in a liquid nitrogen ( $T_m = 77K$ ) Dewar flask and interfaced directly with a PV:HgCdTe photomixer. The cooled IF preamplifier utilized an input impedance matching network and operated over the 10 to 2200 MHz frequency range.

Cooled preamplifiers are not suitable for laser plasma probing applications because they presently do not operate at the liquid helium temperature levels ( $T_m = 4.2K$ ) of extrinsic germanium photomixers. Therefore, cooled impedance matching networks have been developed which transform the photomixer impedance to approximately match the 50-ohm impedance characteristics of the interconnecting transmission line and the IF preamplifier. A microwave network analyzer is employed to determine the real and imaginary components of the photomixer impedance in its operating mode. A cooled microwave matching network which operates over the IF band of interest is then designed and incorporated between the photomixer output and the input to the 50-ohm preamplifier for maximum IF power transfer. A cooled impedance matching network for Ge:Cu photomixers was previously developed (ref. 14) for  $CO_2$  laser radar applications.

A typical matching network for a photomixer with  $R_o = 1200$  ohms\* and  $C_o = 0.05$  pF (fig. 4) utilizes a multipole filter and a quarter-wave transformer type microstrip circuit on an alumina substrate. The cooled matching circuit connects directly to the photomixer. A Kovar housing is employed because of: (1) its similarity to the thermal characteristics of alumina, and (2) its low thermal expansion. These factors are important because of the large amount of temperature cycling that is required between room temperature and liquid helium temperature over a 6 to 12 month test period. A typical block diagram of the  $CO_2$  laser heterodyne receiver is given in figure 5 and a photograph of the receiver package is shown in figure 6. An RFI shielded enclosure and a fiber optic data link are used to minimize RF pickup in the infrared receiver.

## RECEIVER SENSITIVITY MEASUREMENTS

The receiver sensitivity (NEP) has been determined using: (1) an indirect g-r noise measurement technique, and (2) a direct signal-to-noise ratio (SNR) measurement using a blackbody source. The noise measurement technique consists of irradiating the photomixer with the laser LO and measuring the g-r

\* For a 50-ohm IF preamplifier, this represents a VSWR of 24:1. The VSWR is the ratio of the reflected and transmitted waves. Maximum power transfer occurs for VSWR = 1:1.

noise and the receiver thermal noise as a function of applied dc bias (ref. 9). The direct SNR measurement technique (ref. 15) utilizes a spectrally broadband blackbody source and a single frequency laser LO in a heterodyne configuration.

#### 1300-MHZ RECEIVER

The measured heterodyne sensitivity and matching network performance as a function of IF frequency for the 1300-MHz response receiver is given in figure 7. The impedance matching network provides a VSWR of 3:1 between the photomixer and the IF preamplifier over the 400 to 1500-MHz band (fig. 7) and the measured receiver NEP is less than  $2 \times 10^{-19}$  W/Hz over the 300 to 1300 MHz IF frequency range for an applied bias voltage of 10 volts. The upper end of the measured heterodyne response (fig. 7) is limited by the IF amplifier gain roll-off.

#### 2500-MHZ RECEIVER

The measured heterodyne sensitivity and matching network performance as a function of IF frequency for the 2500-MHz response receiver is given in figure 8. The impedance matching network provides a VSWR of 1.5:1 between the photomixer and the IF preamplifier over the 2100- to 2300-MHz band. As can be seen, an NEP  $\approx 2 \times 10^{-19}$  W/Hz was obtained at an IF = 2.3 GHz  $\pm$  200 MHz and the data is in good agreement for the two measurement techniques.

Improved heterodyne receiver sensitivity and higher photomixer gain can be obtained by increasing the dc bias power at the photomixer (equations (1) and (4)). The maximum applied dc bias power ( $P_{dc} = 350$  mW) is fixed by the diameter of the gold wire between the photomixer and the impedance matching network. Receiver sensitivity measurements as a function of dc bias power resulted in a receiver NEP improvement from NEP =  $2 \times 10^{-19}$  W/Hz for  $P_{dc} = 100$  mW, to NEP =  $1.35 \times 10^{-19}$  W/Hz for  $P_{dc} = 250$  mW.

#### 4600-MHZ RECEIVER

The measured heterodyne sensitivity and matching network performance as a function of IF frequency for the 4600-MHz response receiver is given in figure 9. An NEP of  $4.4 \times 10^{-19}$  W/Hz was obtained at an IF of 4.5 GHz for  $P_{dc} = 150$  mW and the IF heterodyne sensitivity is in good agreement with the spectral characteristics of the impedance matching network.

## CONCLUSION

The use of selected wideband germanium photomixers and cooled impedance matching networks has permitted the development of high sensitivity heterodyne receivers with IF responses of 1.3, 2.5, and 4.6 GHz. The heterodyne receivers use microwave techniques to optimize the infrared performance over a specific IF frequency interval and have achieved effective heterodyne quantum efficiencies of: (1)  $\eta' = 30\%$  at IF's which are three times the photomixer 3-dB cutoff frequency, and (2)  $\eta' = 8.5\%$  at IF's which are about six times the photomixer 3-dB cutoff frequency.

The resultant infrared heterodyne receivers have permitted unique  $\text{CO}_2$  laser diagnostic probing measurements of tokamak plasmas. Some initial measurements have resulted in the determination of the penetration depth of the RF heating source and information which is being used to model the interaction mechanism at the turbulent plasma boundary (ref. 3). Plasma ion temperature measurements are presently in progress.

Heterodyne operation at higher IF frequencies, as well as other diagnostic applications, are presently being investigated. The reported impedance matching techniques are believed to be applicable at IF frequencies as high as 8 GHz. In addition, the IF impedance matching techniques are applicable to other types of infrared photomixers.

## REFERENCES

1. Sheffield, J.: Plasma Scattering of Electromagnetic Radiation. Academic Press, 1975.
2. Slusher, R.E. et al.: Bull. Phy. Soc., no. 23, 1976, p. 765.
3. Surko, C.M.; Slusher, R.E.: Study of Driven Lower-Hybrid Waves in the Alcator Tokamak Using CO<sub>2</sub> Laser Scattering. Phys. Rev. Lett. no. 43, 1979, p. 1016.
4. Holzhauer, E.; and Massig, J.H.: An Analysis of Optical Mixing in Plasma Scattering Experiments. Plasma Phys., no. 20, 1978, p. 867.
5. Massig, J.H.: Light Scattering From Thermal Density Fluctuations Using a CW-CO<sub>2</sub> Laser and Heterodyne Detection. Phys. Lett. no. 66A, 1978, p. 207.
6. Wolczok, J.; and Peyton, B.J.: Diagnostic Laser Probing of the Alcator Tokamak. Infrared Phys., no. 19, 1979, pp. 447-454.
7. Kunz, W.: Measurement of Poloidal-Field Induced Faraday Rotation in a Tokamak Plasma. Nuclear Fusion Lett. no. 18, 1978, p. 1729.
8. Slusher, R.E.; and Surko, C.M.: Study of Density Fluctuations in the Absorption of Oxygen on Silicon. Phys. Rev. Lett. no. 40, 1978, pp. 400-403.
9. Arams, F.R.; Sard, E.W.; Peyton, B.J.; and Pace, F.P.: Infrared 10.6 Micron Heterodyne Detection With Gigahertz IF Capability. IEEE J. Quantum Elec., QE-3, 1967, pp. 484-492.
10. Arams, F.R.; Peyton, B.J.; Sard, E.W.; and Pace, F.P.: Semiconductors and Semimetals, Infrared Detectors. Academic Press, NY, vol. 5, 1970, p. 10.
11. Picus, G.S.: Carrier Generation and Recombination Processes in Copper-Doped Germanium Photoconductors. J. Phys. Chem. Solids, no. 23, 1962, p. 1753.
12. Yardley, J.T.; and Moore, C.B.: Response Times of Ge:Cu Infrared Detectors. Appl. Phys. Lett. no. 311, 1965.
13. Peyton, B.J.; Lange, R.A.; Savage, M.; Hoell, J.; and Allario, F.: Remote Airborne Measurements of Stratospheric Ozone, Proceedings of Laser '79 Conference, Orlando, Fla., 1979.
14. Lange, R.A.; Kalisiak, P.; Rubinstein, I.; and Pace, F.P.: 10.6 Micron Heterodyne Monopulse Receiver with Doppler Tracking Capability. IEEE J. of Quantum Elec., QE-9, 1973.



REFERENCES (continued)

15. Peyton, B.J.; DiNardo, A.J.; Cohen, S.C.; McElroy, J.H.; and Coates, R.J.: An Infrared Heterodyne Radiometer for High-Resolution Measurements of Solar Radiation and Atmospheric Transmission. IEEE J. of Quantum Elec., QE-11, 1975.

TABLE I. MEASURED Ge:Cu(Sb) PHOTOMIXER CHARACTERISTICS

Mixer operator temperature, $T_m$ .....	4.2K
Electric field, E .....	500 V cm <sup>-1</sup>
3-dB cutoff frequency, $f_c$ .....	800 MHz
Power handling capability .....	500 mW
Carrier lifetime, $\tau$ .....	$2 \times 10^{-10}$ sec
Mixer dc resistance, $R_o$ .....	1200 ohms (with LO applied)
Quantum efficiency, $\eta$ .....	0.55
Photo gain, $\tau/T$ .....	0.011

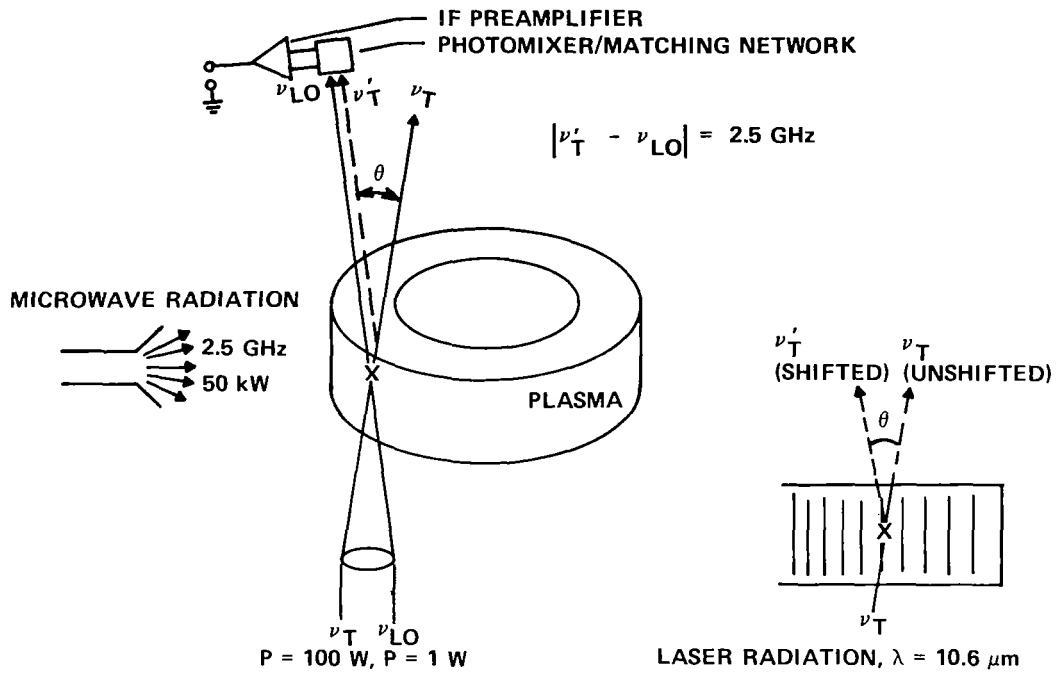


Figure 1.- Plasma probing technique.

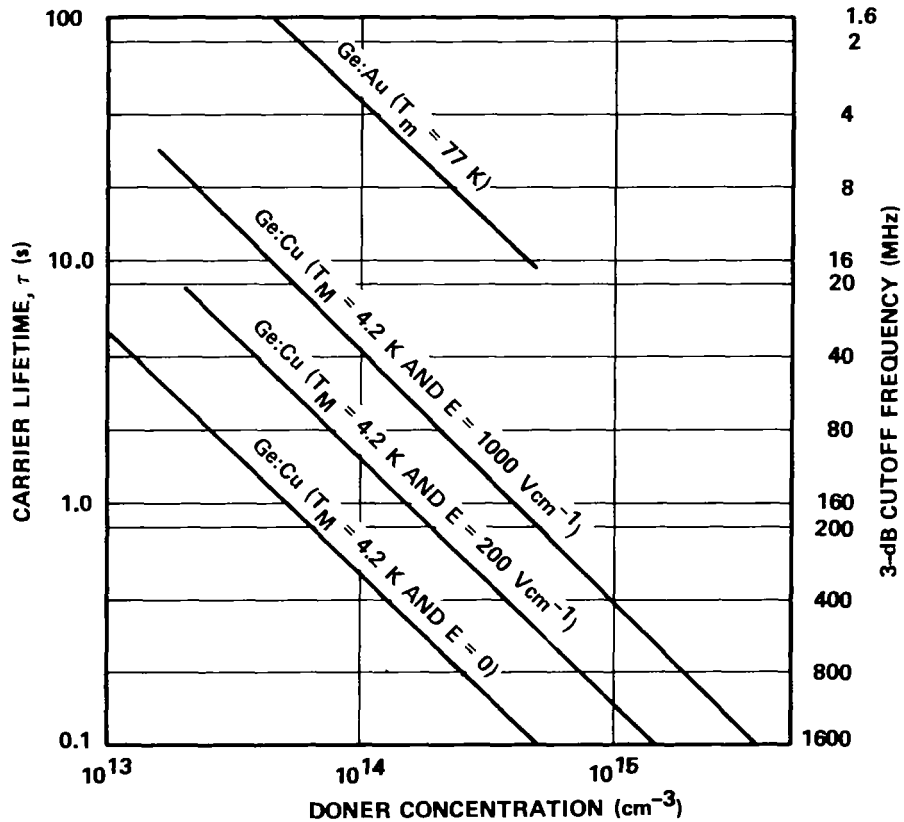


Figure 2.- Measured variation of carrier lifetime with donor concentration for extrinsic germanium photoconductors.

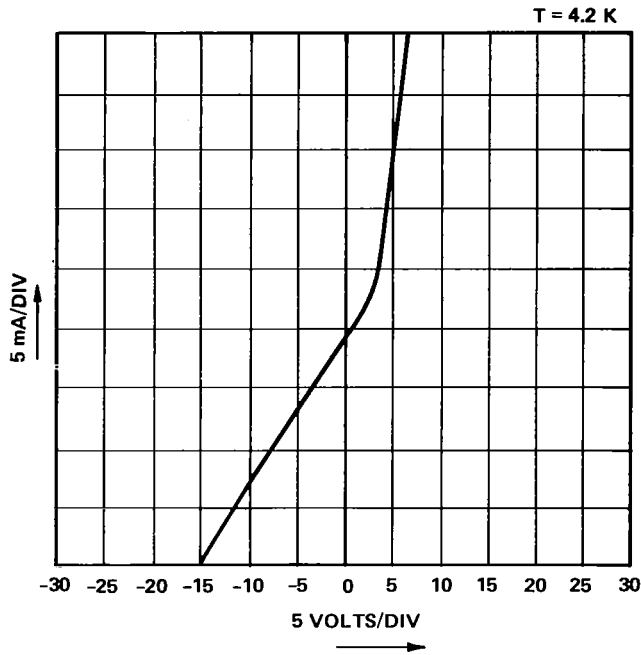
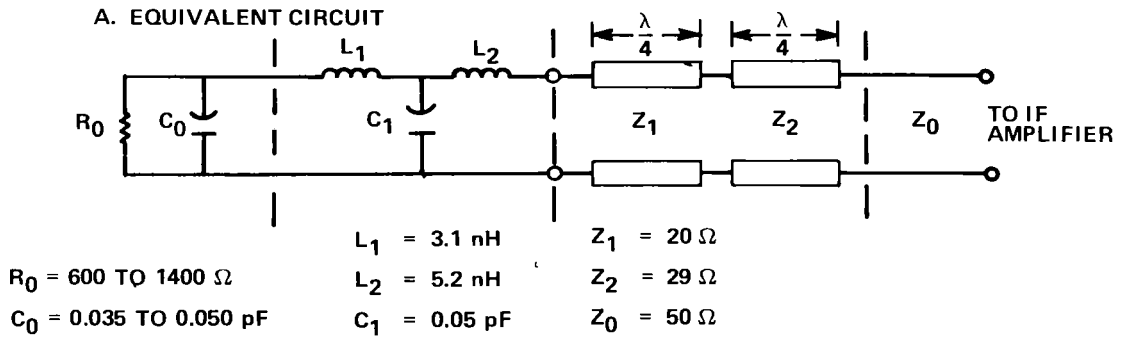


Figure 3.- I-V characteristics of Ge:Cu(Sb) photomixer.



B. PHOTOMIXER/MATCHING NETWORK MOUNT

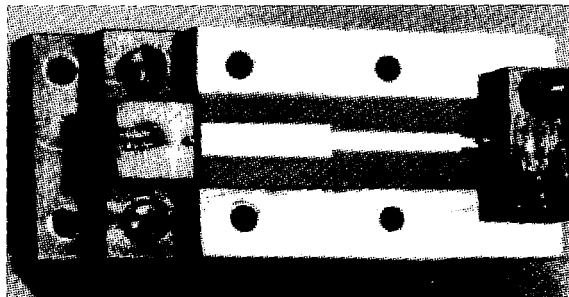


Figure 4.- Cooled mixer impedance matching network for 2.5-GHz infrared heterodyne receiver.

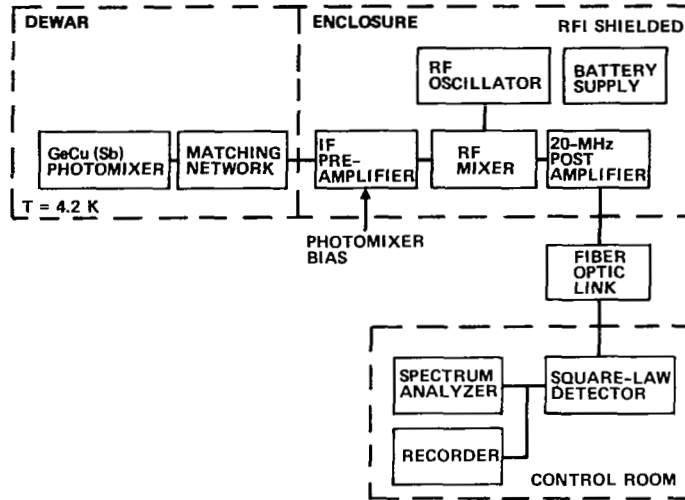


Figure 5.- CO<sub>2</sub> laser infrared heterodyne receiver for lower hybrid heating diagnostics.

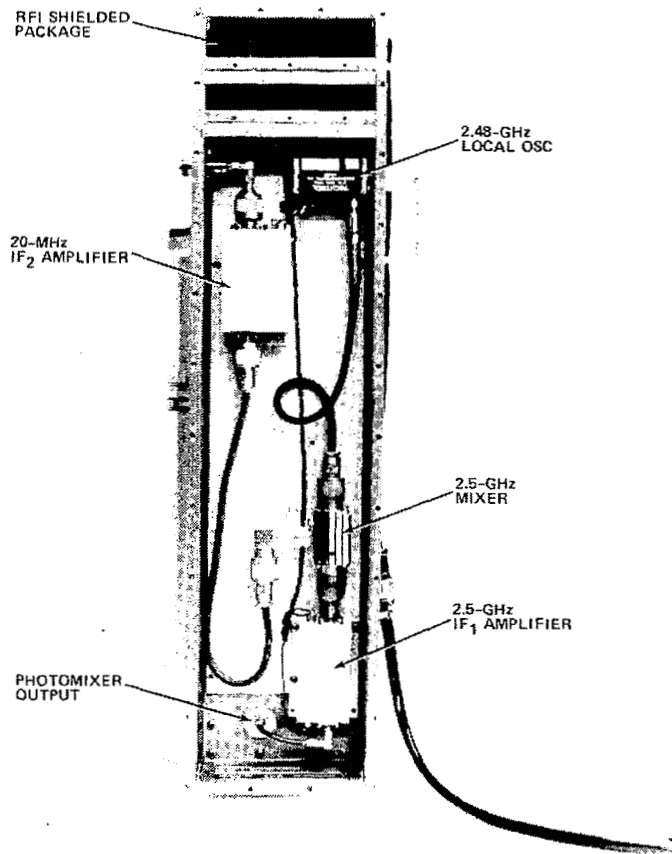


Figure 6.- Packaged infrared heterodyne receiver for lower hybrid heating diagnostics.

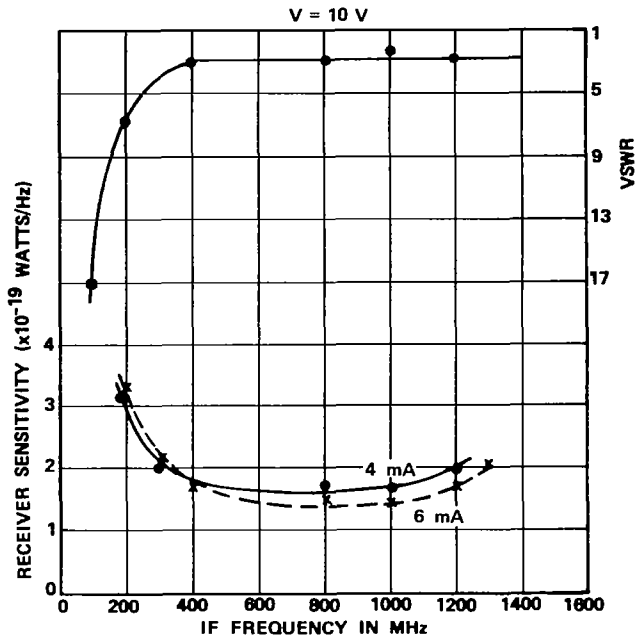


Figure 7.- Measured NEP and matching network performance versus IF frequency for 1300 MHz response infrared heterodyne receiver.

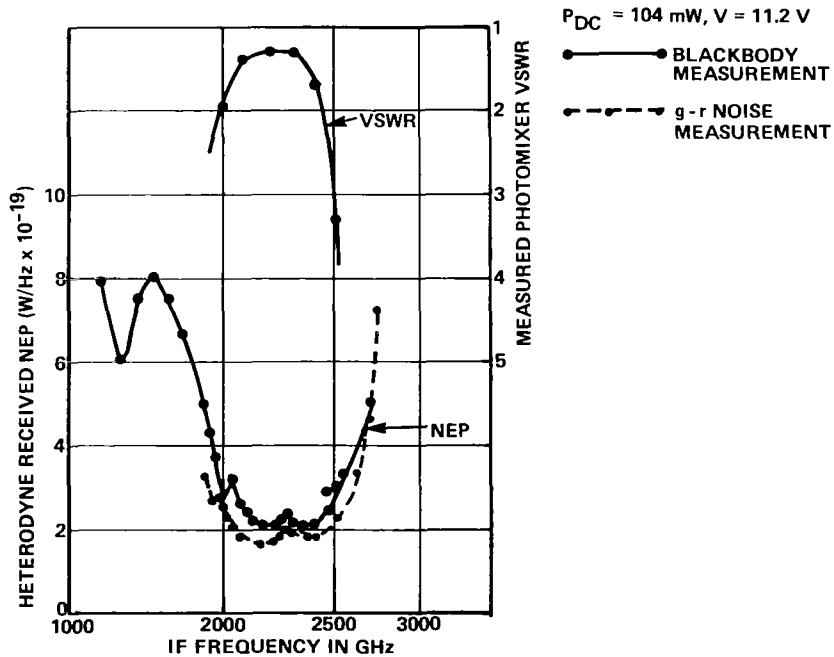


Figure 8.- Measured heterodyne receiver sensitivity versus IF frequency.

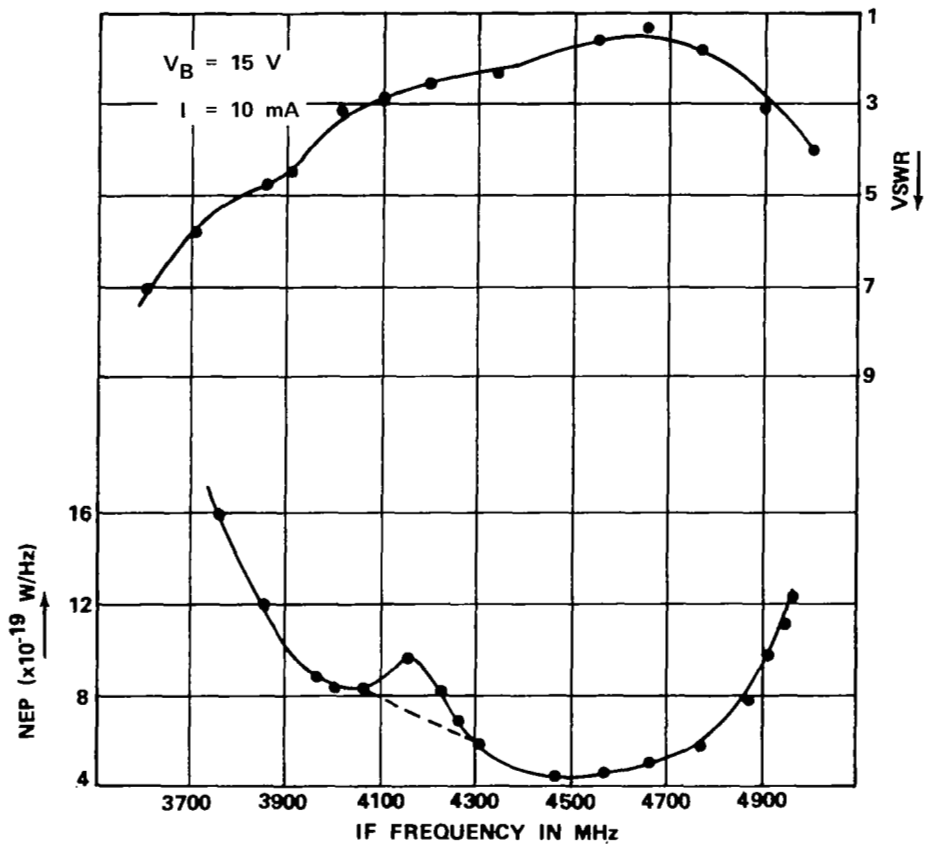


Figure 9.- Measured NEP and matching network performance for 4600 MHz response infrared heterodyne receiver.